Hindawi Publishing Corporation
Advances in Mechanical Engineering
Volume 2014, Article ID 371403, 18 pages
http://dx.doi.org/10.1155/2014/371403

Research Article

Collaborative Synchronization Digital Control for Double Hydraulic Cylinders

Zhi-hao Liu, Qin-he Gao, Chuan-qiang Yu, Xiang-yang Li, Wen-liang Guan, and Gang-feng Deng

Xi'an Research Institution of High Technology, Xi'an 710025, China

Correspondence should be addressed to Chuan-qiang Yu; fishychq@163.com

Received 8 April 2014; Revised 12 July 2014; Accepted 24 July 2014; Published 1 September 2014

Academic Editor: Long Cheng

By researching the synchronization motion of double hydraulic cylinders controlled by high-speed on-off valve, the paper aims to solve the shortage of current hydraulic synchronization system with low synchronization precision. The flow characteristic of high-speed on-off valve with pulse width-frequency modulation is researched compared with pulse width modulation. The mathematical equations of the double hydraulic cylinders are formulated with bulk-cavity-node method in MATLAB/Simulink. The collaborative synchronization control is analyzed and the compound algorithm of collaborative synchronization control and pulse width-frequency modulation is simulated compared with collaborative synchronization control. The hydraulic loop is set up to verify the simulation result with the proposed control algorithm on the FESTO platform. The research finds that (1) the pulse width-frequency modulation control can be linear to the flow of high-speed on-off valve on the duty bound of 0~100%; (2) the collaborative synchronization control is effective to eliminate the displacement error between the double cylinders which results from the different load environment and other disturbance.

1. Introduction

Synchronization motion of hydraulic system is widely used in the fields of military and industrial manufacturing [1] and the precision of synchronization motion influences the system performance directly.

High precision synchronization motion of the hydraulic system is usually realized by proportional valve or servo valve [2], while the proportional or servo valve has many disadvantages, such as weak antipollution ability and being controlled indirectly by PC. In order to decrease the cost and complexity, high-speed on-off valve (HSV) is proposed with the advantage of low-cost, compact structure, antipollution, high speed responsibility, adjusted by pulse, and so forth [3]. HSV has been used in many situations, for example, pressure control [4] and position control [5]. With the mechanical and electromagnetic inertia leading the flow delay, many researchers have applied some methods to deal with the flow delay. Taghizadeh et al. [6] use the linear compensation method to achieve closed loop position control by widening the duty ratio based on the switching parameters with the frequency fixed. Sorli and Pastorelli [7] use the modified differential pulse width modulation (PWM) method to control the position of a pneumatic rod-less cylinder. Qin et al. [8] research the pulse frequency modulation (PFM) control method to compensate the dead zone and applied to the speed control for the hydraulic motor, which achieves the speed control. To solve the flow delay, the pulse width-frequency modulation (PWM-PFM) is presented, which can be referred to as the changed frequency and changed duty ratio of HSV.

To gain the better synchronization performance, synchronization control algorithms are researched by many researchers for the high synchronization precision. Synchronization control methods can be ranked by the interrelation of multiactuators as 3 different types [9]: equivalent control, master-slave control, and collaborative control. Fang et al. [10] designed the equivalent controls to control, respectively, the two cylinders of the rolling mill on the process of rapid

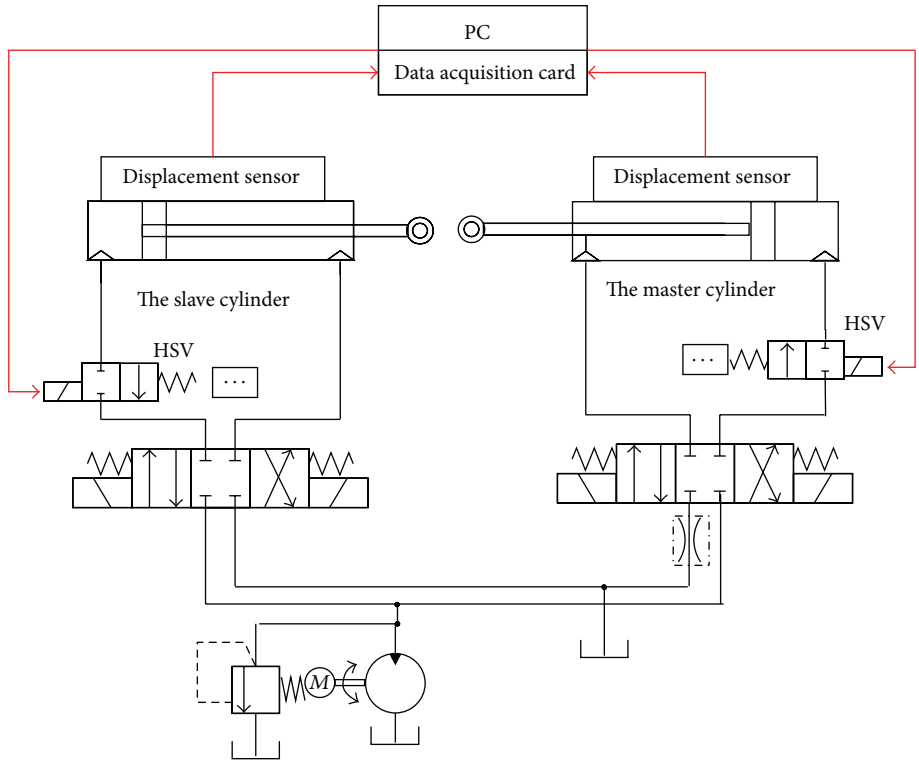

Figure 1: Scheme figure of the collaborative synchronization control system.

Figure 2: Hydraulic loop of the double hydraulic cylinders system.

milling; however, the different performances between the two cylinders were not taken into consideration to be compensated in the equivalent control method. Liu [11] designed a high precision hydraulic lifting by utilizing master-slave control method with the right cylinder tracking the displacement of the left cylinder to modify the synchronization error. The master-slave control can realize the synchronization control effectively, but this control approach may cause the surge of the slave cylinder because the slave cylinder is controlled based on the difference of displacement, which might be influenced by the noise. Mastellone et al. [12] designed the collaborative synchronization control for the base joint of dexterous robot hand and proposed the synchronization position error feedback theory, which decreases the synchronization error to realize the synchronization control. In order to improve the synchronization precision of the double hydraulic cylinders, the synchronization control algorithm, combining position control of the single cylinder and synchronous control of the double cylinders, is proposed and researched. With the timely feature of the feedforward control and the anti-interference of the feedback control, the compound algorithm of speed feedforward and displacement PI feedback is used for the position control and the fuzzy algorithm is utilized for the synchronization control with its intelligent interference.

The main contributions of this paper are the following.

(1) The PWM-PFM for HSV is proposed to settle the flow delay resulting from the mechanical and electromagnetic inertia and the flow characteristic of HSV with PWM-PFM is analyzed compared with PWM.

(2) Collaborative synchronization control algorithm is researched and the compound algorithm of Collaborative synchronization control and PWM-PFM is verified by simulation and experiment.

The rest of the paper is organized as follows. The dynamic of the double hydraulic cylinders, including HSV and the double hydraulic cylinders, is analyzed and presented in Section 2, "*Dynamic of the Hydraulic System*" section. The collaborative synchronization control is presented in Section 3, "*Analysis and Simulation of Collaborative Synchronization Control*" section. PWM-PFM is proposed to compensate the dead zone and utilized to the collaborative synchronization control, which is presented in Section 4, "*Collaborative Synchronization Control and PWM-PFM*".

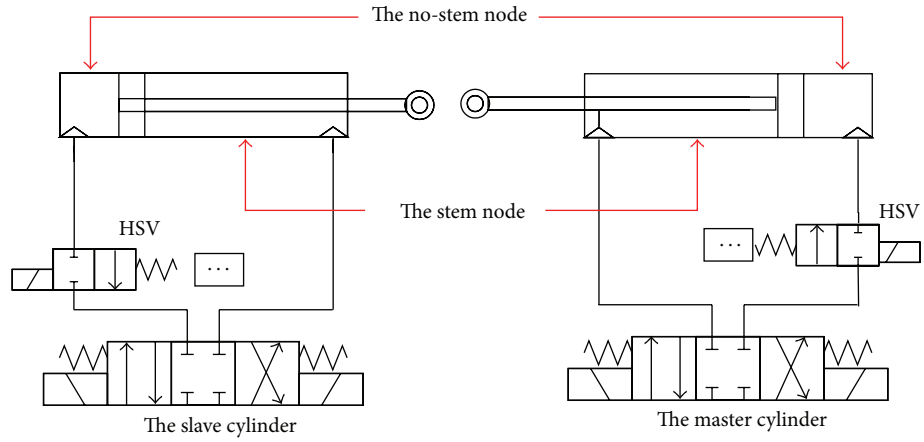

Figure 3: Schematic diagrams of bulk-cavity-node method.

Section 5, "*Experimental Verification*" section, verifies the proposed control algorithm by experiment. Finally, the study is ended with several concluding remarks of the research work.

2. Dynamic of the Hydraulic System

The scheme figure of the collaborative hydraulic control system is presented in Figure 1, which is mainly composed of a personal computer (PC) with the data acquisition card PCI-6221, the displacement sensors for the hydraulic cylinders, HSVs, and three position four-way reversing valves and some accessories (Figure 2).

The displacement sensors are installed to measure the displacements of the hydraulic cylinders gathered by the AI ports of PCI-6221 data acquisition card. HSV controls the flow to the no-stem cavity of hydraulic cylinder by adjusting the open time of HSV. HSV is controlled by the amplified PWM signal, which was produced by the AO port of data acquisition card.

2.1. Mathematical Model of Double Hydraulic Cylinders. The flow equations of the hydraulic system is formulated with the bulk-cavity-node method [13] shown in (1), which illuminates the relationship between the pressure and the total flow:

$$P = \int \frac{E_0}{V} \sum Q_i dt, \tag{1}$$

where $\sum Q_i$ is the total flow of the cavity; P is the pressure of the cavity; E_0 is the elastic modulus of oil; V is the volume of no-stem cavity.

The nodes of double hydraulic cylinder are divided into two parts according to hydraulic system schematic diagram (Figure 3): stem nodes and no-stem nodes.

Flow equations of the double hydraulic cylinders are as follows:

(1) the stem node of the slave cylinder

$$\frac{dp_{zy}}{dt} = \frac{\beta_e}{V_{zy0} - A_{zy}x_z}\left(A_{zy}\dot{x}_z + Q_{zx} - Q_{z\text{out}}\right), \tag{2}$$

where p_{zy} is the pressure of the stem cavity, V_{zy0} is the initial volume of the stem cavity, A_{zy} is the effective area of the stem cavity, Q_{zx} is the flow that leaks from the stem cavity to no-stem cavity, and $Q_{z\text{out}}$ is the flow that flows out of the no-stem cavity;

(2) the no-stem node of the slave cylinder

$$\frac{dp_{zw}}{dt} = \frac{\beta_e}{V_{zw0} + A_{zw}x_z}\left(Q_{\text{hsv1}} - A_{zw}\dot{x}_z - Q_{zx}\right), \tag{3}$$

where p_{zw} is the pressure of the no-stem cavity, V_{zw0} is the initial volume of the no-stem cavity, A_{zw} is the effective area of the no-stem cavity, and Q_{hsv1} is the flow that flows into the stem cavity of the slave cylinder;

(3) the rod node of the master cylinder

$$\frac{dp_{yy}}{dt} = \frac{\beta_e}{V_{yy0} - A_{yy}x_y}\left(A_{yy}\dot{x}_y + Q_{yx} - Q_{y\text{out}}\right), \tag{4}$$

where p_{yy} is the pressure of the stem cavity, V_{yy0} is the initial volume of the stem cavity, A_{yy} is the effective area of the stem cavity, Q_{yx} is the flow that leakage from the stem cavity to no-stem cavity, and $Q_{y\text{out}}$ is the flow that flows out of the no-stem cavity;

(4) the rod-less node of the master cylinder

$$\frac{dp_{yw}}{dt} = \frac{\beta_e}{V_{yw0} + A_{yw}x_y}\left(Q_{\text{hsv2}} - A_{yw}\dot{x}_y - Q_{yx}\right), \tag{5}$$

where p_{yw} is the pressure of the no-stem cavity, V_{yw0} is the initial volume of the no-stem cavity, A_{yw} is the effective area of the no-stem cavity, and Q_{hsv2} is the flow that flows into the stem cavity of the master cylinder.

Force balance equations of the double hydraulic cylinders are as follows:

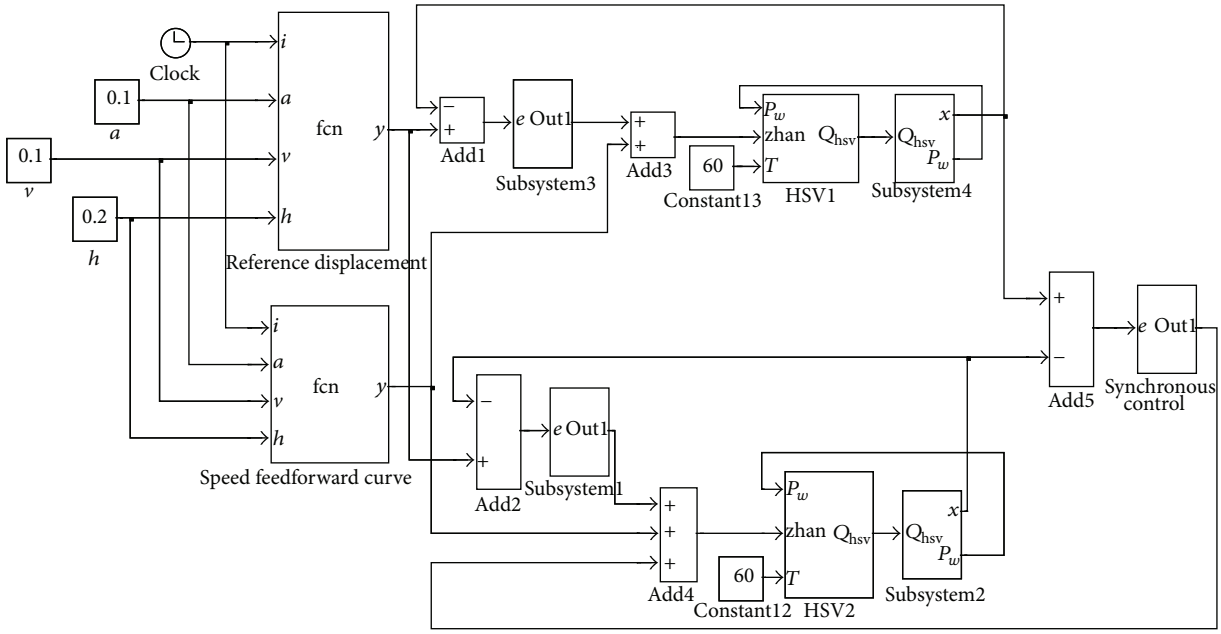

Figure 4: Mathematical model of the double hydraulic cylinder.

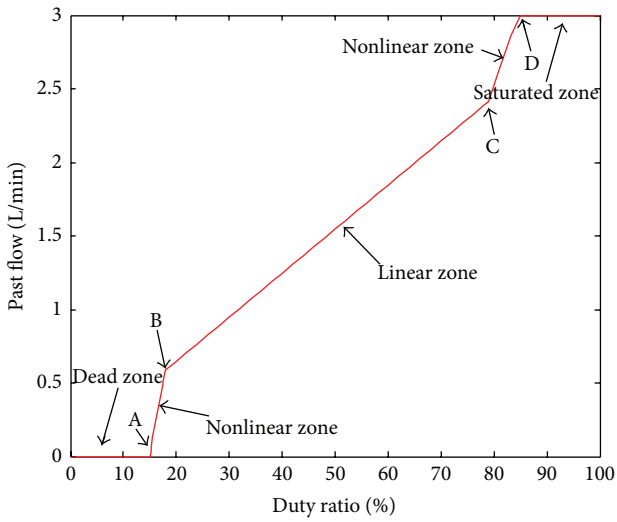

Figure 5: Flow characteristic of HSV.

(1) force balance equation of the slave cylinder

$$m_z\ddot{x}_z = p_{zw}A_{zw} - p_{zy}A_{zy} - \beta_{zc}\dot{x}_z, \tag{6}$$

where m_z is the equivalent piston mass of the slave cylinder and β_{zc} is viscous damping coefficient of oil;

(2) force balance equation of the master cylinder

$$m_y\ddot{x}_y = p_{yw}A_{yw} - p_{yy}A_{yy} - \beta_{yc}\dot{x}_y, \tag{7}$$

where m_y is the equivalent piston mass of the master cylinder and β_{yc} is viscous damping coefficient of oil.

The assistant equations of the hydraulic synchronization system are shown in the following:

$$\begin{aligned} &Q_{zin} + Q_{yin} = C, \qquad F = k\delta + c\dot{\delta}, \\ &Q_{zout} = C_d A_v \sqrt{\frac{2}{\rho} p_{zy}}, \qquad Q_{yout} = C_d A_v \sqrt{\frac{2}{\rho} p_{yy}}, \\ &Q_{zx} = k_{zx}\left(p_{zw} - p_{zy}\right), \qquad Q_{yx} = k_{yx}\left(p_{yw} - p_{yy}\right), \end{aligned} \tag{8}$$

where C is the flow of the constant-source hydraulic pump; k_{zx} is the leakage flow coefficient of the left cylinder and k_{yx} is the leakage flow coefficient of the right cylinder; F is the crashing force; k is the severity of the string; c is the damping coefficient; δ is the creep length of the contactor.

Mathematical equations ((2)~(8)) are modeled in MATLAB/Simulink (Figure 4).

2.2. Mathematical Model of HSV. In order to use the discrete HSV instead of continuous proportional and servo valves and to obtain the similar linear flow characteristic, PWM techniques are used and on-off signal with PWM techniques is applied as the control input to control HSV [14]. The fluid which passed through the HSV is delivered to the hydraulic cylinder as discrete packets. If PWM frequency is faster than the dynamic of the hydraulic cylinder and load, the system would filter the discreteness of the packets and respond to the average of the input signal similar to the continuous case.

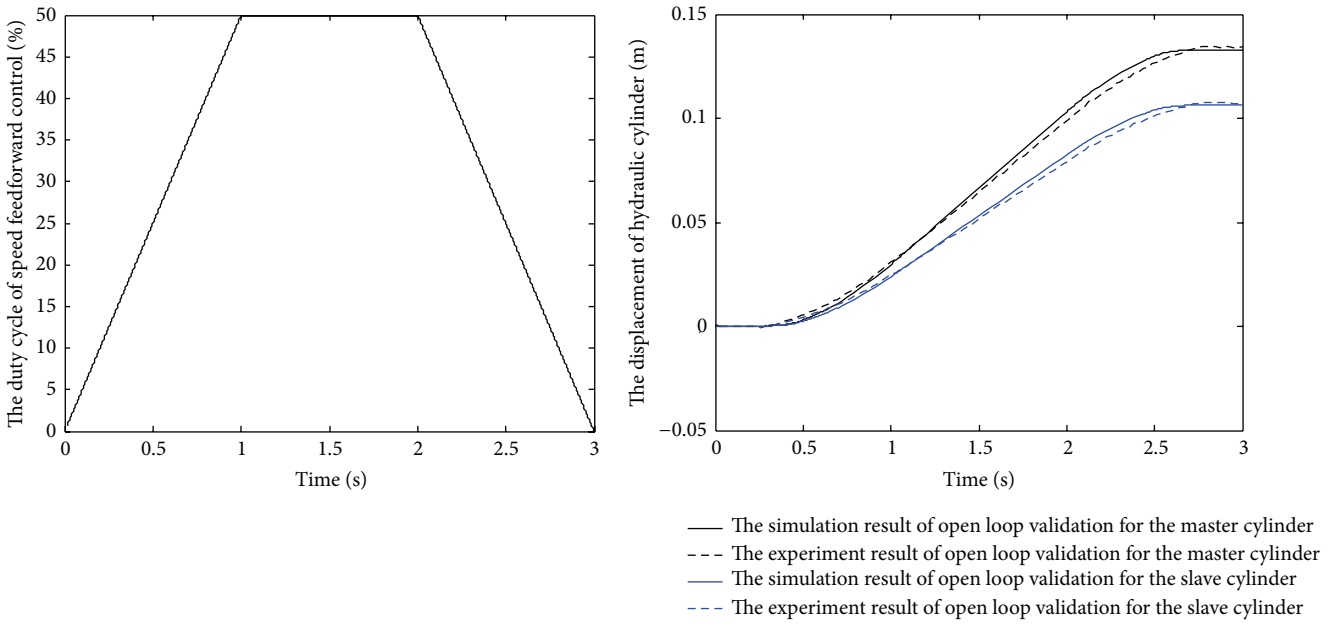

(a) Duty ratio of HSV

(b) Displacement of the double cylinders

FIGURE 6: Model validation.

Because of the mechanical and electromagnetic inertia, the spool average displacement [15] is formulated as follows:

$$\overline{x}_{\mathrm{hsv}} = \begin{cases} 0 & \tau \in [0, \tau_1) \\ \frac{1}{2}\left(\frac{\tau_2+\tau_4}{\tau_2^2}\right)\left(\tau+\tau_{yc1}-\tau_1\right)^2 x_{vm} & \tau \in [\tau_1, \tau_{12}) \\ \left[\left(\frac{\tau_2+\tau_3}{\tau_2}\right)\tau-\tau_1-\frac{\tau_2}{2}+\frac{\tau_4}{2}-\frac{\tau_1\tau_3}{\tau_2}\right]x_{vm} & \tau \in [\tau_{12}, \tau_{\mathrm{on}}) \\ \left(\tau+\tau_3-\tau_1+\frac{\tau_4-\tau_2}{2}\right)x_{vm} & \tau \in [\tau_{\mathrm{on}}, 1-\tau_{\mathrm{off}}) \\ \left(\tau+\tau_3-\tau_{yc2}+\frac{\tau_4-\tau_2}{2}\right)x_{vm} & \tau \in [1-\tau_{\mathrm{off}}, \tau_{34}) \\ \left[1-\frac{\left(\tau+\tau_3-\tau_{yc2}-1\right)^2}{2\tau_4}-\frac{\tau_2\left(\tau+\tau_3-\tau_{yc2}-1\right)^2}{2\tau_4^2}\right]x_{vm} & \tau \in [\tau_{34}, 1-\tau_3) \\ x_{vm} & \tau \in [1-\tau_3, 1], \end{cases} \tag{9}$$

where t_1 is the time of electromagnetic delay, $t_1 = 2.5$ ms; t_2 is the time of starting, $t_2 = 0.5$ ms; t_3 is the time of power-off delay, $t_3 = 2.5$ ms; t_4 is the time of moving reversely, $t_4 = 1$ ms; T is the period of the PWM signal, $T = 1/30$ s; $\tau_1 = t_1/T$; $\tau_2 = t_2/T$; $\tau_3 = t_3/T$; $\tau_4 = t_4/T$; $\tau_{yc1} = (\tau-\tau_1)\tau_3/\tau_2$; $\tau_{yc2} = (1-\tau-\tau_3)\tau_1/\tau_4$; $\tau_{12} = \tau_1 + \tau_2^2/(\tau_2+\tau_3)$; $\tau_{34} = 1-\tau_3-\tau_4^2/(\tau_1+\tau_4)$; $\tau_{\mathrm{on}} = \tau_1+\tau_2$; $\tau_{\mathrm{off}} = \tau_3+\tau_4$; x_{vm} is the maximal displacement of the spool; $\overline{x}_{\mathrm{hsv}}$ is the average displacement of the spool.

As a ball valve, the average area of valve opening [16] is formulated in the following:

$$\overline{A}_{\mathrm{hsv}} = \frac{\pi D \overline{x}_{\mathrm{hsv}} \sin(2\theta)}{2}, \tag{10}$$

where $\overline{A}_{\mathrm{hsv}}$ is the average valve-port area of HSV; D is the diameter of valve ball, $D = 0.005$ m; θ is the half-angle of valve seat, $\theta = 20$ deg; $\overline{x}_{\mathrm{hsv}}$ is the average displacement of valve ball.

The flow rate of HSV is formulated assuming turbulent flow as

$$Q_{\mathrm{hsv}} = C_d \overline{A}_{\mathrm{hsv}} \sqrt{\frac{2\left(p_y - p_w\right)}{\rho}}, \tag{11}$$

where Q_{hsv} is flow that through HSV; C_d is flow coefficient; p_y is pressure of rod cavity, $p_y = 3.5$ MPa; p_w is pressure of no-stem cavity; ρ is oil density, $\rho = 850$ Kg/m3; $\tau_1 = t_1/T$.

The model of past flow characteristic is simulated in MATLAB/Simulink and the simulation result is shown in Figure 5.

Figure 5 shows that (1) the past flow has linear relationship with the duty ratio within the range 18%~79%, on occasion of the mechanical and electromagnetic inertia.

(2) When the duty ratio is under 15%, the past flow is zero as the motion of spool is delayed and the spool is closed.

(3) When the duty ratio is with the bound of 18%~21%, the spool cannot be open absolutely.

(4) When the duty ratio is within the bound of 79%~85%, the spool cannot be closed absolutely.

(5) When the duty ratio exceeds 85%, the past flow is maximal as the spool remains open.

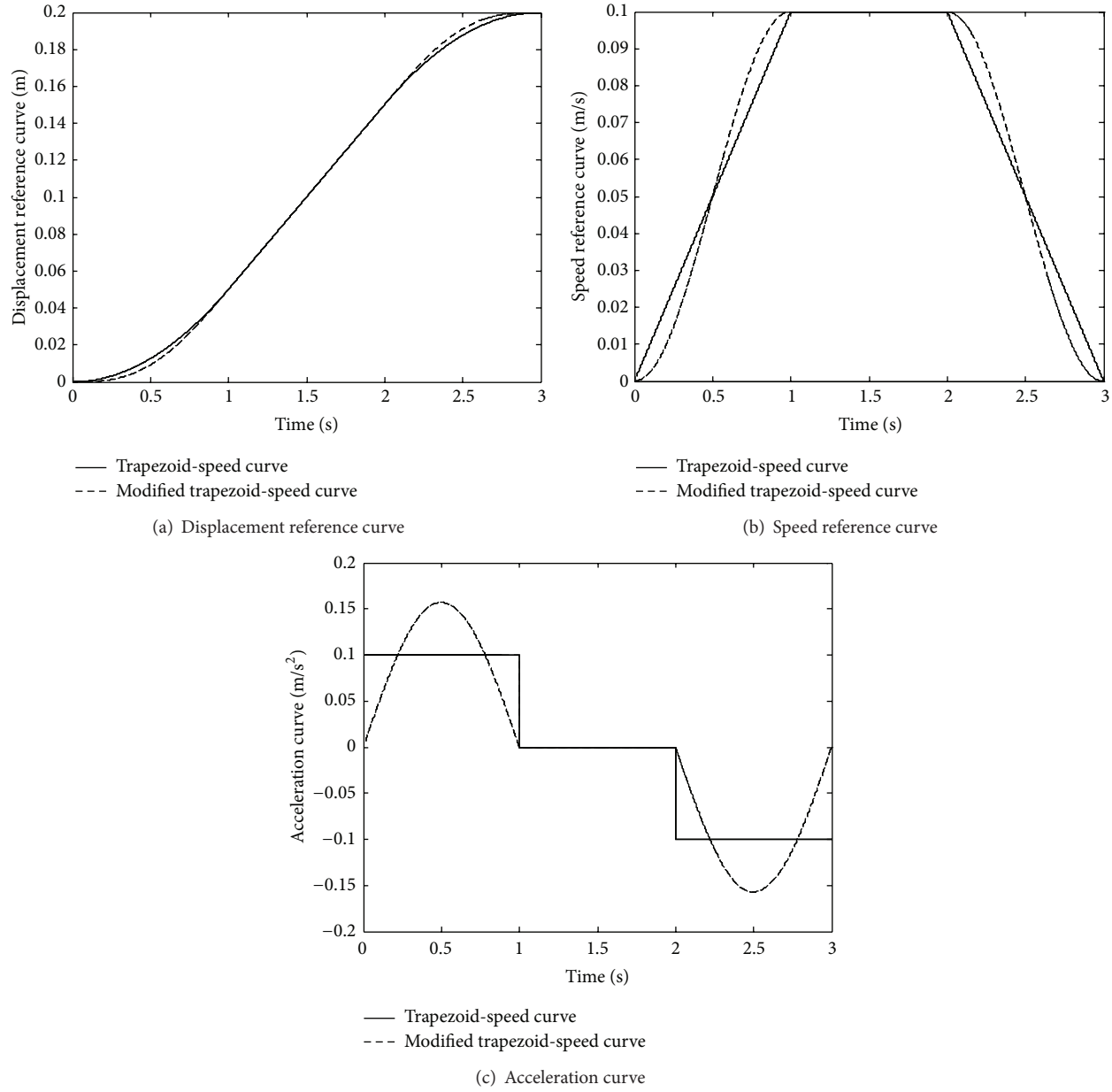

(a) Displacement reference curve

(b) Speed reference curve

(c) Acceleration curve

Figure 7: Speed feedforward and displacement feedback signal.

The result implies that the switching characteristic parameter affects directly the flow characteristic of HSV. Dead zone, saturated zone, and nonlinear zone become bigger as switching characteristic parameters of HSV get bigger with frequency of pulse signal fixed. The minimal responding duty ratio of HSV is $dc_{\min} = (t_1 + t_2)/T$ and the maximal responding duty ratio is $dc_{\max} = 1 - ((t_3 + t_4)/T)$.

2.3. Model Validation. The parameters of mathematical model are evaluated as Table 1.

The experiment is implemented to validate the mathematical model by comparing the simulated and experimental displacement of the double hydraulic cylinders. The trapezoid duty ratio of PWM signal for HSV presented in Figure 6(a) shows that the maximum duty ratio is 50% and the rate of change is 50%/s.

The experiment and simulation (Figure 6(b)) show that (1) the displacement error of the simulation and experiment exists in the start process for the slave or master cylinders resulting from the changed flow dead zone of HSV. The changeable pressure leads to the instability switching parameters which results from the different flow dead zone, while the switching parameters of simulating environment are fixed.

(2) The displacement error of the simulation and experiment exists in the end process for the slave or master cylinders resulting from the changed flow saturated zone of HSV.

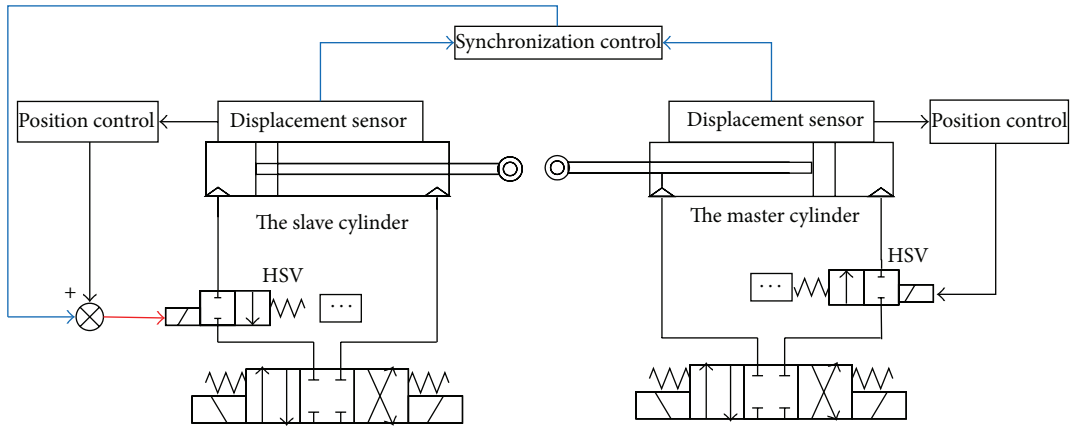

Figure 8: Collaborative synchronization control algorithm.

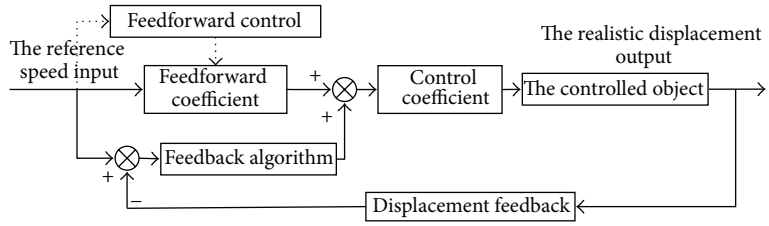

Figure 9: SFDF algorithm.

The changeable pressure leads to the instability switching parameters which results from the different flow saturated zone, while the saturated zone of simulation is fixed.

(3) The displacement of the double hydraulic cylinders is different from each other, mainly for the different structure and load environment.

2.4. Trajectory Planning. In order to avoid the oscillatory of the hydraulic cylinders, the trapezoid-speed curve is usually used as the speed reference [17], while the acceleration curve of the trapezoid-speed curve is discrete, which may cause the oscillatory at the end of the accelerated section and the start of descended section. The modified trapezoid-speed curve is designed to avoid the breaking acceleration (Figure 7(c)) and the speed reference curve and displacement reference curve are shown in Figures 7(a) and 7(b).

3. Analysis and Simulation of Collaborative Synchronization Control

3.1. Analysis of Collaborative Synchronization Control. The collaborative synchronization control algorithm is presented to increase the synchronization precision, which is divided into two parts: the position control of the each single cylinder and the synchronization control of the double cylinders (Figure 8).

The position control algorithm of single cylinder aims to eliminate the error between the real displacement and reference trajectory and the synchronization control algorithm is used to wipe out the error between the double cylinders resulted from different characteristics and different load environments.

3.1.1. Position Control Algorithm. The compound algorithm of speed feedforward and displacement PI feedback (SFDF) is proposed as the position control algorithm of the single cylinder, which is shown in Figure 9. SFDF algorithm makes use of the timely feature of the feedforward control and the anti-inference ability of the feedback control.

The PI feedback algorithm is utilized to compensate the error between the displacement input reference and the realistic output to deal with the uncertainties associated with the hydraulic system and the speed feedforward is multiplied by the PI feedback control. The final duty ratio of the pulse signal can be defined in the following:

$$e = x_1 - x_2,$$

$$u_{\mathrm{PI}}(k) = K_p e(k) + K_{ia} \sum_{i=1}^{k} e(j)\, T = K_p e(k) + K_i \sum_{i=1}^{k} e(j),$$

$$u(t) = k_2 \left[k_1 * v_{\mathrm{ideal}}(t) + u_{\mathrm{PI}}(t) \right], \tag{12}$$

where $u_{\mathrm{PI}}(t)$ is the output of displacement PI feedback; x_1 is the reference displacement; x_2 is the realistic displacement of hydraulic cylinder; $K_i = K_{ia}T$; K_p is the proportional coefficient; K_{ia} is the integral coefficient; T is sampling period; k is sampling serial number; k_2 is the PI control coefficient; k_1 is the speed feedforward coefficient.

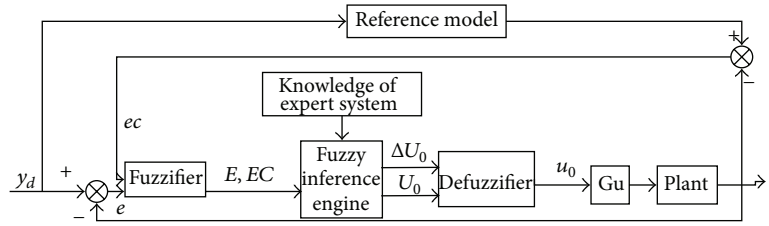

Figure 10: Structure of fuzzy control.

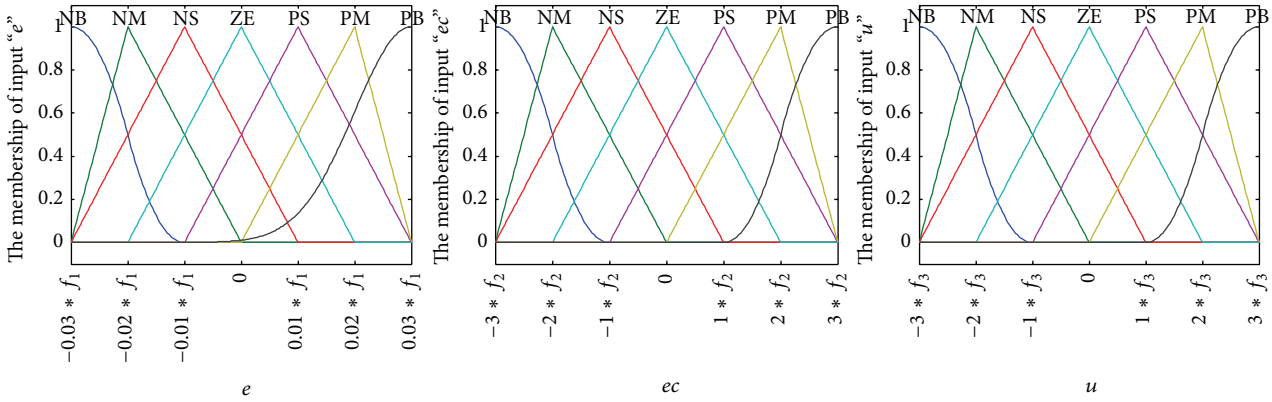

Figure 11: Memberships of the input and output for the fuzzy algorithm.

3.1.2. Fuzzy Control. The fuzzy control is utilized to compensate the displacement error of the double hydraulic cylinders and as the core of the synchronous control, the fuzzy control is composed of fuzzier, fuzzy inference engine and defuzzier [18].

The structure of the fuzzy controller determines the control performance and the complexity of the system and MISO type fuzzy control; the error between the double cylinders and the derivation of error being the input of the fuzzy controller and the duty ratio of the pulse signal being the output of the fuzzy controller are designed (Figure 10).

(1) Fuzzier of Input Variables. The basic ranges of input and output variables are $e \in [-0.03 * f_1, 0.03 * f_1]$, $ec \in [-3 * f_2, 3 * f_2]$, and $u \in [-3 * f_3, 3 * f_3]$ and the input is transformed into proper semantic value with fuzzification. The fuzzy ranges of input and output are both separated into 7 semantic variables, respectively, and the corresponding fuzzy subsets are

$$e, ec, u = [\text{NB}, \text{NM}, \text{NS}, \text{ZO}, \text{PS}, \text{PM}, \text{PB}], \quad (13)$$

where NB is negative big; NM is negative middle; NS is negative small; ZO is zero; PS is positive small; PM is positive middle; PB is positive big.

Let NB and PB be gauss membership functions and others are triangular membership functions. All variables of the membership functions are shown in Figure 11.

(2) Establishment of Fuzzy Inference Rule. The key to realize fuzzy control is to establish appropriate fuzzy inference rules by using the experience of experts. The fuzzy inference rules between input e, ec and output u are summarized in Table 2 for the stability, response frequency, and steady-state precision of the electrohydraulic system.

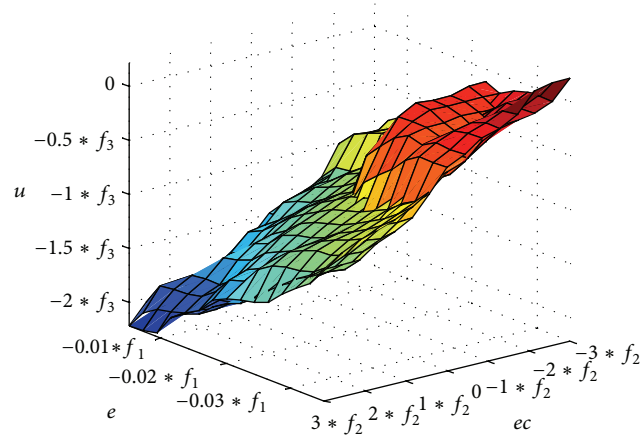

Figure 12: Control area of fuzzy block.

The control area of the fuzzy block between the input and the output is shown in Figure 12.

(3) Defuzzier. The fuzzy implication and synthesis calculation are carried out by the Mamdani min and max operators, respectively. Thus, the result of u [19] is

$$\mu_{C_j}(u) = \bigvee_{i,j=1}^{7} \left\{ \left[\mu_i(e) \wedge \mu_j(ec) \right] \wedge \mu_{ij}(u) \right\}. \quad (14)$$

Table 1: Component parameters of the double hydraulic cylinders.

Parameters	Value	Parameters	Value	Parameters	Value
β_e	750 MPa	m_z m_g	9 kg	A_{zy} A_{gy}	0.005 m^2
p_{zp} p_{gp}	7 MPa	β_c	250 N·s/m	k_c	0.0033 m^3/(Pa·s)
ρ	850 kg/m^3	V_{zy0} V_{gy0}	28.275 mm^3	A_{zw} A_{gw}	0.002 m^2
x_{zxc} x_{gxc}	0.2 m	V_{zw0} V_{gw0}	56.965 mm^3		

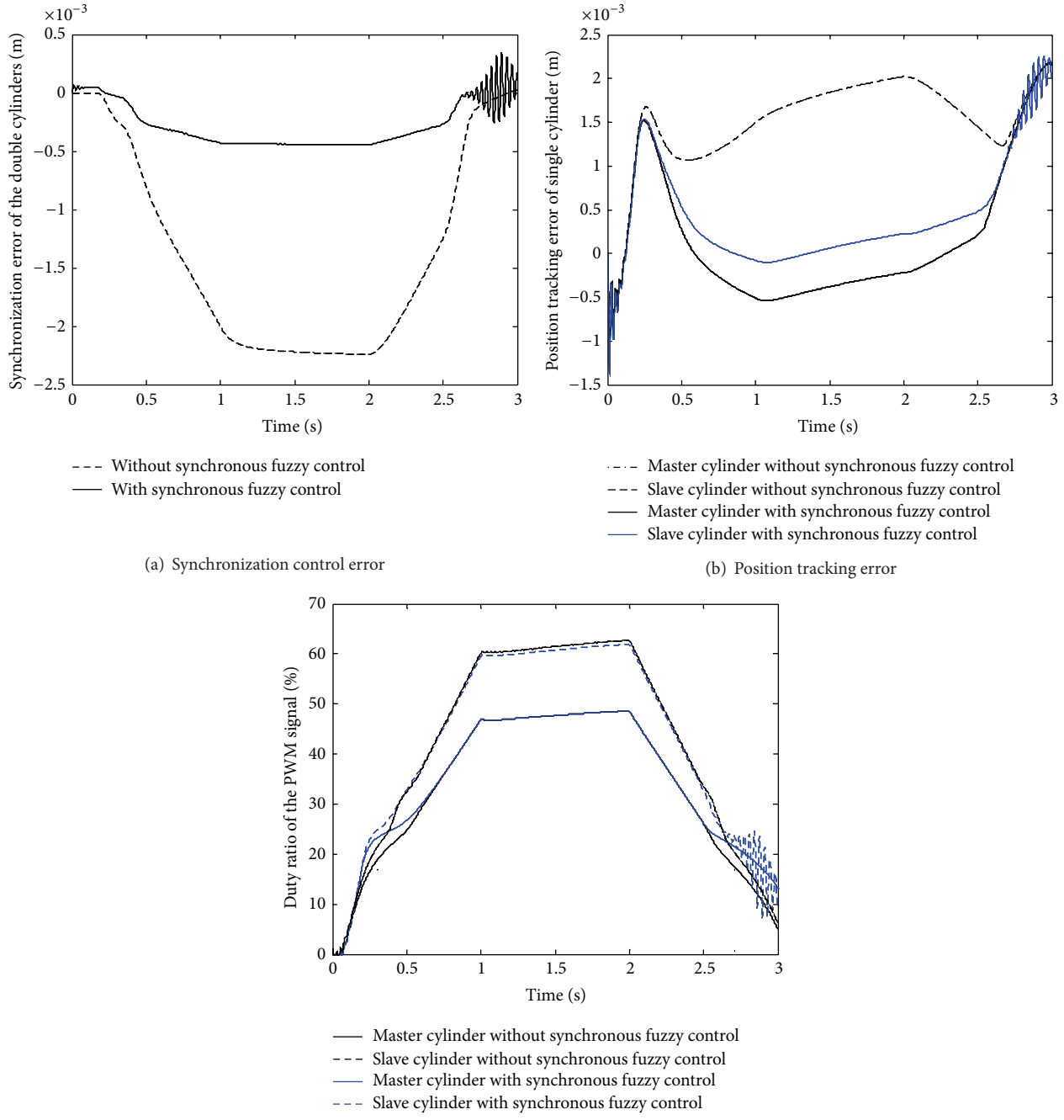

Figure 13: Simulation of collaborative synchronization control.

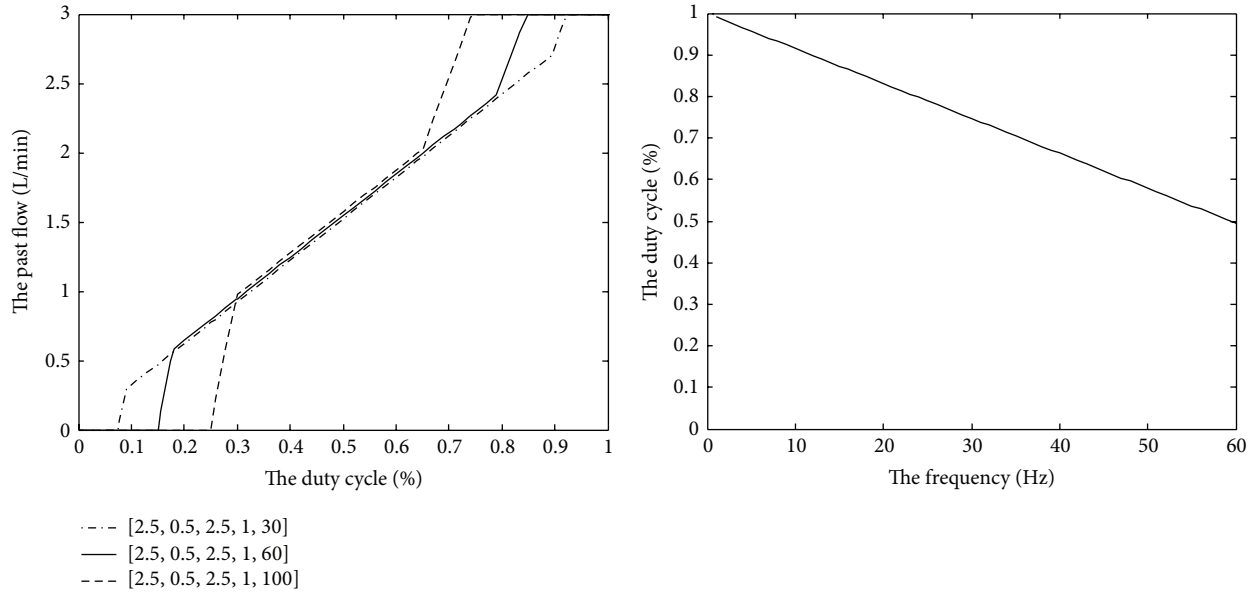

(a) Flow characteristic of HSV

(b) Flow linear zone

Figure 14: Flow characteristic of HSV with different frequency.

Table 2: Tables of fuzzy inference rule.

e/*ec*	NB	NM	NS	ZE	PS	PM	PB
NB	NB	NB	NM	NM	NS	ZE	ZE
NM	NB	NB	NM	NS	NS	ZE	PS
NS	NB	NM	NS	NS	ZE	PS	PS
ZE	NM	NM	NS	ZE	PS	PM	PM
PS	NM	NS	ZE	PS	PS	PM	PB
PM	ZE	ZE	PS	PS	PM	PB	PB
PB	ZE	ZE	PS	PM	PM	PB	PB

The centroid method [20] is used to implement defuzzification after the output fuzzy set u is acquired from the fuzzy operation. The duty ratio u is obtained as follows:

$$u(e, ec) = \frac{\sum_{n=1}^{N} u_n \mu_{C_j}(u)}{\sum_{n=1}^{N} \mu_{C_j}(u)}. \quad (15)$$

The proportion coefficient of the fuzzy range can influence the dynamic characteristic of the system and is regulated with the offline regulation method, which is shown in Table 3.

3.2. A Step by Step Procedure to Execute Collaborative Synchronization Control

Step 1. Initialize parameters a, v, and s, and give the speed feedforward curve and the displacement feedback curve of the double cylinders, respectively.

Step 2. Detect displacement of the mater hydraulic $x_1(t)$ with the displacement sensor and read $x(t)$ $v_{\text{ideal}}(t)$ based on the t, calculate the error $e_1(t) = x_1(t) - x(t)$ and the PI feedback algorithm $u_1(k)$, and add $v_{\text{ideal}}(t) * k_1$ and $u_1(k)$ as the control output to achieve the position control of the master hydraulic cylinder.

Table 3: List of proportion coefficient of the fuzzy range.

Parameters	*e*	*ec*	*u*
Lingual parameters	Error	The derivation of error	The duty ratio
Proportion coefficient	K_e	K_{de}	K_u

Step 3. Detect displacement of the slave hydraulic $x_2(t)$ with the displacement sensor and read $x(t)$ $v_{\text{ideal}}(t)$ based on the t, calculate the error $e_2(t) = x_2(t) - x(t)$ and the PI feedback algorithm $u_1(k)$, and add $v_{\text{ideal}}(t) * k_1$ and $u_2(k)$ as the control output to achieve the position control of the slave hydraulic cylinder.

Step 4. Calculate the synchronization error $e_2(t) = x_2(t) - x(t)$ and calculate the membership of $e_2(t)$ and the control output U_{fuzzy} based on the fuzzy interference.

Step 5. Add U_{fuzzy} to $u_2(k)$ as the control output of the slave cylinder, control the duty ratio of the high-speed on-off valve with the control output, and control the hydraulic cylinder indirectly.

Step 6. Return Step 2.

3.3. Simulation of Collaborative Synchronization Control. The parameters are initialized with $K_e = 60$, $K_{de} = 5$, and $K_u = 0.1$ to verify the effect of synchronization control for double

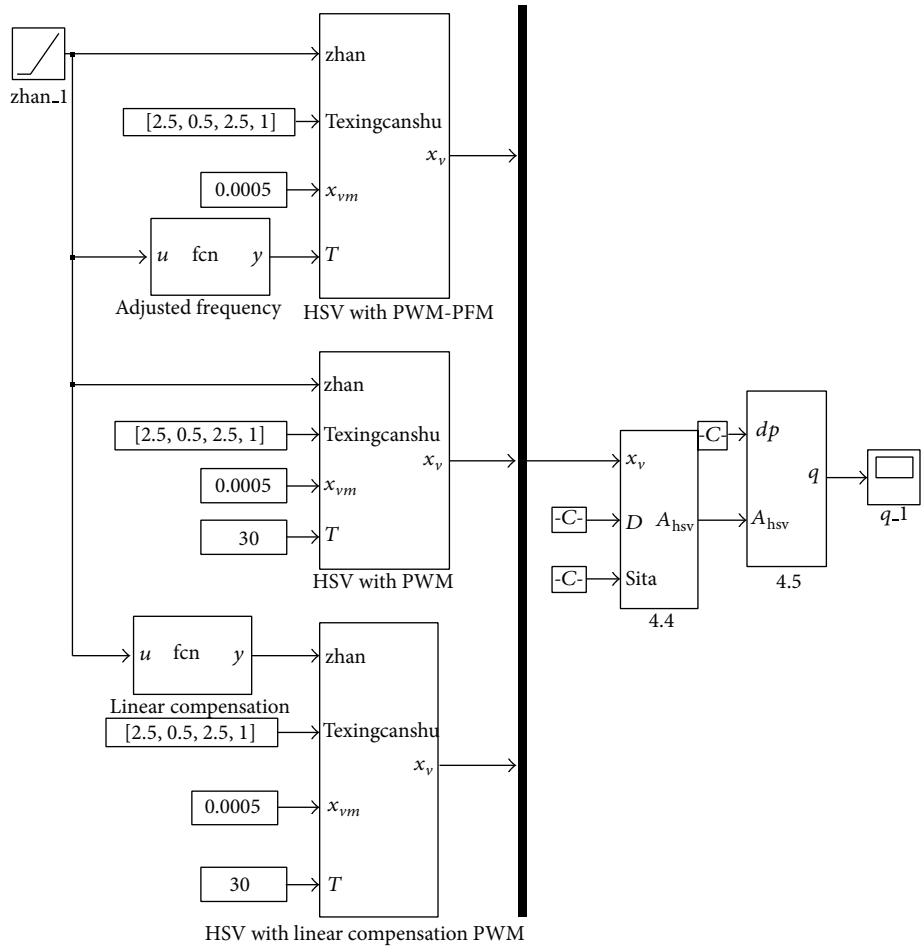

Figure 15: Mathematic model of HSV with PWM-PFM compared with PWM.

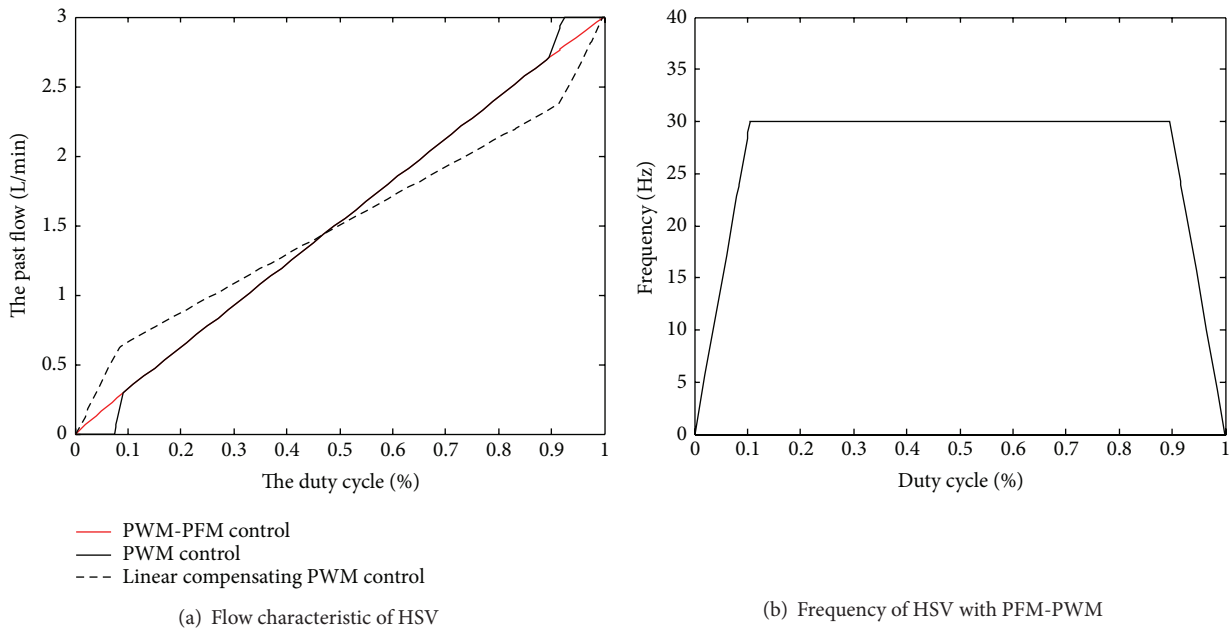

(a) Flow characteristic of HSV

(b) Frequency of HSV with PFM-PWM

Figure 16: Flow characteristic of PWM-PFM control.

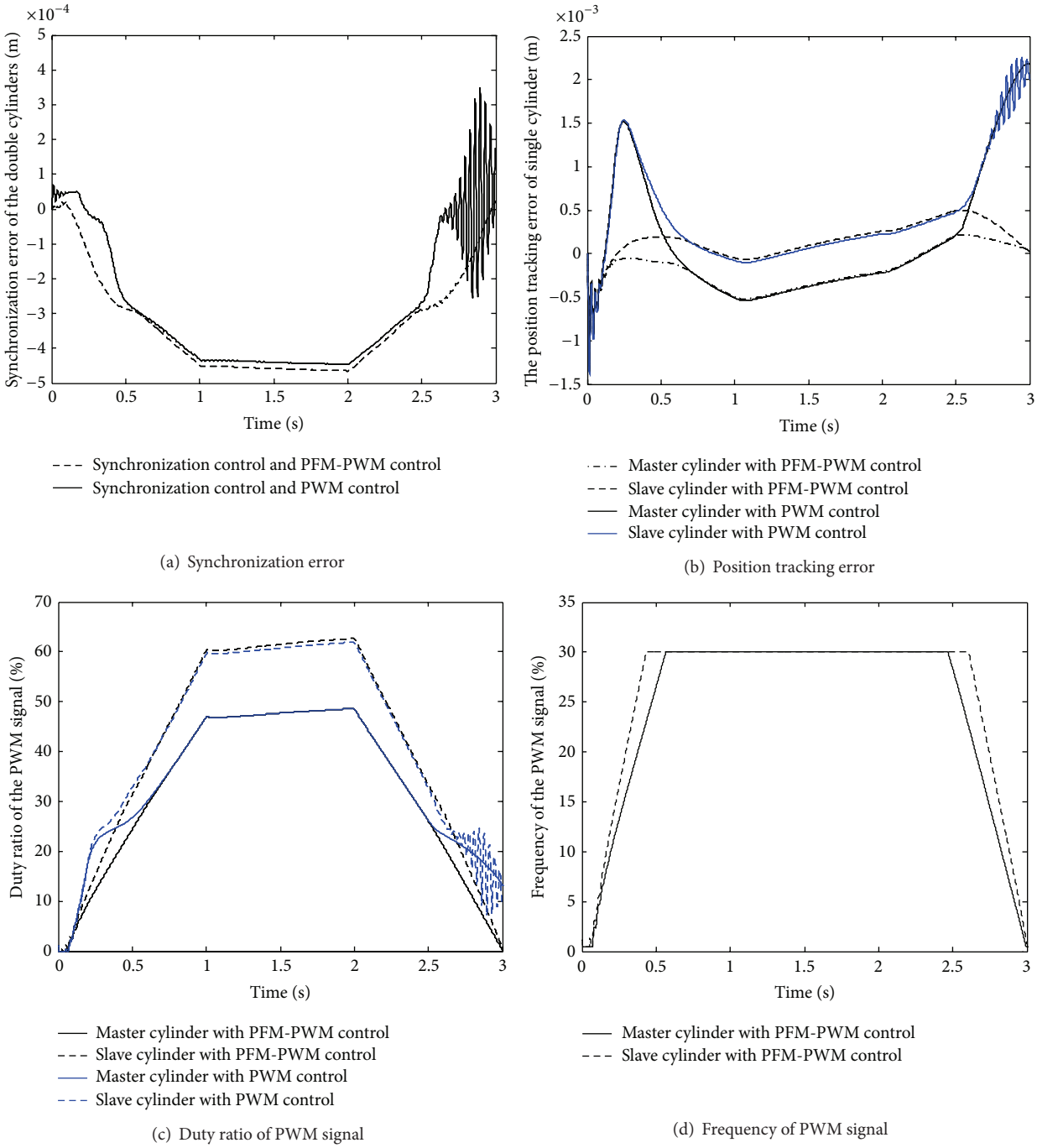

Figure 17: Collaborative synchronization control and PWM-PFM.

hydraulic cylinders system. The simulation is compared with the synchronization control without the fuzzy control shown in Figure 13. The tracking error of the single cylinder, the duty ratio of the master and slave hydraulic cylinders, and the displacement error of the double cylinders are listed to compare with each other.

Figure 13 shows the following. (1) The larger position tracking error is presented at the start process (Figure 13(b)) resulting from the dead zone of the HSV, and the flow cannot reach the control required when the duty ratio is under the minimal responding duty ratio of HSV.

(2) The larger position tracking error and oscillatory is presented at the end process resulting from the saturated zone of the HSV and the flow cannot reach the control required when the duty ratio exceeds the maximum responding duty ratio of HSV.

(3) The synchronization control with fuzzy algorithm has a better performance than that of synchronization control

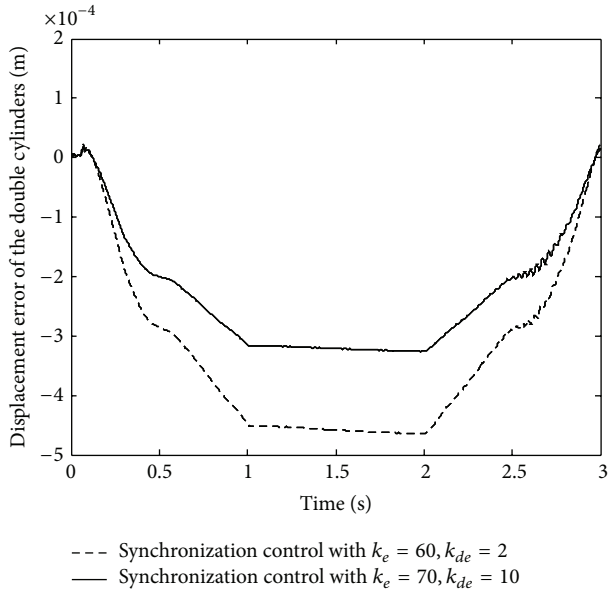

Figure 18: Synchronization control with different control parameters.

without fuzzy algorithm and decreases the maximal error from 2.3 mm to 0.4 mm, which verifies the effectiveness of the collaborative synchronization algorithm.

(4) Despite the better performance of the fuzzy control for the synchronization control, the oscillatory also exists, especially at the end of the process (Figures 13(a) and 13(c)), which reveals the limit of the PWM for HSV.

4. Collaborative Synchronization Control and PWM-PFM

The analysis shows that the oscillatory and the larger tracking error results from the flow dead zone with the small duty ratio and flow saturated zone with the large duty ratio (Figures 5 and 13). In order to compensate the flow dead zone and the saturated zone, some research has been forced on the nonlinear characteristic, such as the linear compensation PWM [6] and the differential PWM [7]. In this paper, the PWM-PFM control algorithm is proposed to decrease the position error controlled for the larger tracking error and the oscillatory.

4.1. Flow Characteristic of HSV with PWM-PFM. In order to validate the PWM-PFM control, the flow characteristic of HSV with different frequency is researched. Mathematical model is simulated with the initial parameters $[t_1, t_2, t_3, t_4] = [2.5, 0.5, 2.5, 1]$, $f = 30/60/100$, and the flow characteristic and the linear zone with different frequency is shown in Figure 14.

The simulation shows that (1) the dead zone of HSV with 30/60/100 Hz is (0~7.5)%, (0~15)%, and (0~25)%, respectively.

(2) The nonlinear zone of HSV with 30/60/100 Hz is (7.5~10.5)% and (89.5~92.5)%, (15~18)% and (82~85)%, and (25~30)% and (70~75)%, respectively.

(3) The linear zone of HSV with 30/60/100 Hz is (10.5~89.5)%, (18~82)%, and (30~70)%, respectively.

(4) The saturated zone of HSV with 30/60/100 Hz is (92.5–100)%, (85–100)%, and (75–100)%, respectively.

The result implies that the dead and sutured zone gets larger as the frequency of the pulse signal becomes bigger while the linear zone decreases.

The PWM-PFM control deals with the dead and saturated zone by adjusting the frequency as the duty ratio changes, which changes the frequency with the same width of pulse signal.

The minimal responding duty ratio of HSV is shown in

$$\tau_{\min} = \frac{t_1 + t_2}{T}. \tag{16}$$

For some small duty ratio under the minimal responding duty ratio, the maximum frequency of HSV calculated from (16) is shown in

$$f = \frac{\tau}{t_1 + t_2}. \tag{17}$$

The maximum responding duty ratio of HSV is shown in

$$\tau_{\max} = 1 - \frac{t_3 + t_4}{T}. \tag{18}$$

For some duty ratio exceeding the maximum responding duty ratio, the minimal frequency of HSV calculated from (18) is shown in

$$f = \frac{1 - \tau}{t_3 + t_4}. \tag{19}$$

The adjusted frequency can be concluded with (16)~(19). Consider

$$f = \begin{cases} \dfrac{\tau}{t_1 + t_2} & \tau \in \left[0, \dfrac{(t_1 + t_2)}{T}\right) \\ \dfrac{1}{T} & \tau \in \left[\dfrac{(t_1 + t_2)}{T}, \dfrac{(t_3 + t_4)}{T}\right) \\ \dfrac{1 - \tau}{t_3 + t_4} & \tau \in \left[\dfrac{(t_3 + t_4)}{T}, 1\right). \end{cases} \tag{20}$$

The equation is adjusted with the switching parameters $t_1 = 2.5$ ms, $t_2 = 0.5$ ms, $t_3 = 2.5$ ms, $t_4 = 1$ ms, and $T = 1/30$ and the frequency for PWM-PFM control is shown in

$$f = \begin{cases} \dfrac{\tau}{0.003} & x \in [0, 0.09) \\ 30 & x \in [0.09, \quad 0.895) \\ \dfrac{1 - \tau}{0.0035} & x \in [0.895, 1). \end{cases} \tag{21}$$

Mathematic equation (21) of HSV with PWM-PFM is modeled in MATLAB/Simulink compared with that with PWM (Figure 15).

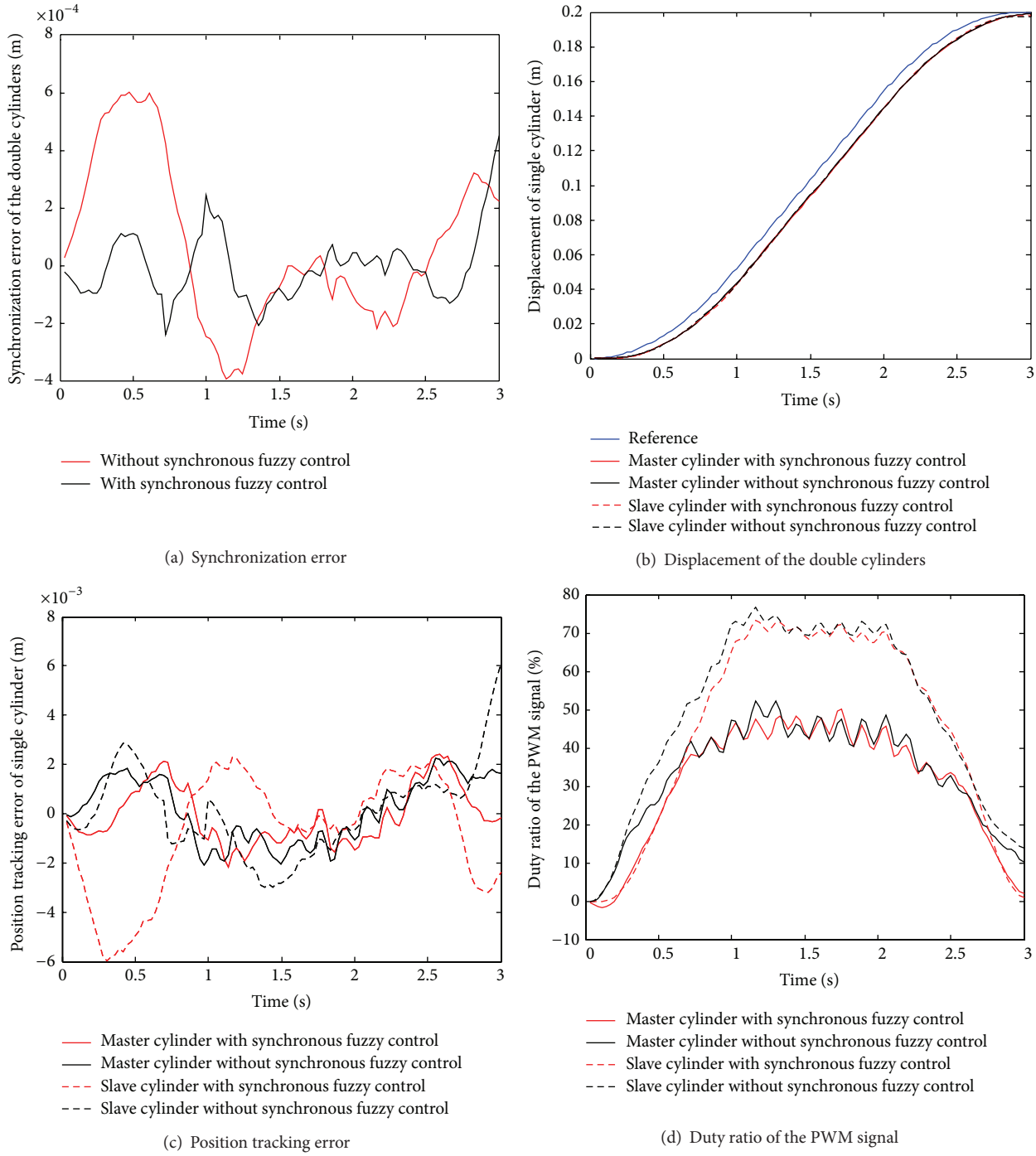

FIGURE 19: Experimental verification of collaborative synchronization control.

PWM-PFM control is verified with the simulation of the flow characteristic for HSV compared with the PWM control and the linear compensation PWM [6] control (Figure 16).

Figure 16 illustrates that (1) the linear compensation PWM can avoid the dead and saturated zone, while changing the flow characteristic (Figure 16(a)); (2) the dead zone, nonlinear zone, and saturated zone is compensated by the changeable frequency and the flow characteristic is unchanged.

The result (Figure 16) shows that the PWM-PFM for HSV can compensate the dead zone, nonlinear zone, and saturated zone resulting from the mechanical structure and make the flow linear on the duty ratio bound of [0 ~ 100%].

4.2. Simulation of Collaborative Synchronization Control and PWM-PFM. Collaborative synchronization control and PWM-PFM is used to decrease the position tracking error

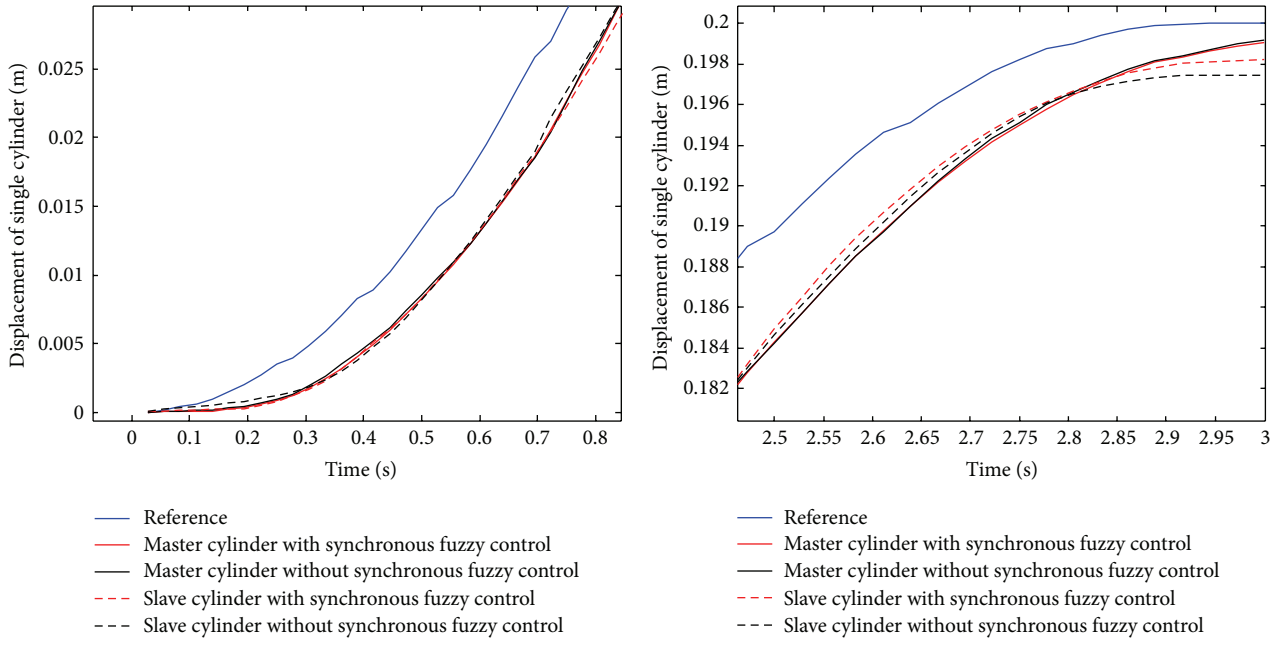

Figure 20: Magnified displacement of the single cylinder.

and avoid the oscillatory which result from the dead and saturated zone of HSV. The synchronous process of the double hydraulic cylinders is simulated and the position tracking error, synchronization error, frequency, and duty ratio of PWM signal are presented in Figure 17.

Figure 17 shows that (1) the larger tracking error is eliminated with PWM-PFM of HSV and the tracking error is decreased from 2.5 mm to 0.5 mm (Figure 17(b)) by adjusting the frequency according to (21) (Figure 17(d)).

(2) The oscillatory of the displacement of the hydraulic (Figure 17(b)) and the control signal (Figure 17(c)) is eliminated with the changeable frequency.

(3) The linear flow controlled by the PWM-PFM of HSV can eliminate the vibration of the synchronization control, and the PWM-PFM control algorithm has a better performance than the PWM control algorithm by adjusting the control gain on the basis of the stabilization of the system which is illustrated in Figure 18.

Figure 18 shows that the synchronization error is decreased from 0.5 mm to 0.2 mm with adjusting the control parameters $K_e = 70$, $K_{de} = 10$, and $K_u = 0.1$.

The result shows that HSV with PWM-PFM can keep the hydraulic system with the larger gain which ensures the high precision synchronization control.

5. Experimental Verification

The synchronization motion experiment of double hydraulic cylinders is done to verify the collaborative synchronization control on the FESTO hydraulic platform with the system pressure setting 6 MPa. The sample rate of the displacement signal is 1 KHZ, and the rate of control algorithm is 10 HZ.

Two normally closed HSV (HSV-3101S1) produced by Gui-Zhou automotive electronic control technology co. are used to control the flow of the master and slave cylinders, respectively. With NI data acquisition device gathering displacement signals of two cylinders, the system is realized with LABView for programming the collaborative synchronization control and MATLAB for analyzing the data.

5.1. Collaborative Synchronization Control. The collaborative synchronization control is verified by comparing with synchronization control without fuzzy control. The experimental result is shown in Figure 19, and in order to distinguish the difference between the collaborative synchronization control and the synchronization control without synchronous control clearly, the magnified displacement of the start and end process is presented in Figure 20.

Figures 19-20 show that (1) the collaborative synchronization control can decrease the synchronous error from 0.6 mm to 0.3 mm (Figure 19(a)) resulting from the different system structure and load environment.

(2) The steady error of the position tracking exists, mainly for the dead zone, nonlinear zone, and saturated zone of flow control. HSV with PWM cannot reach the control requirement for the nonlinear flow characteristic.

The result shows that the collaborative synchronization control presents a better synchronous performance, while there is some room to be upgraded.

5.2. Collaborative Synchronization Control and PFM-PWM. Since the flow characteristic of HSV with PWM-PFM control is analyzed and simulated in Section 4.1, the experimental verification of collaborative synchronization and PWM-PFM

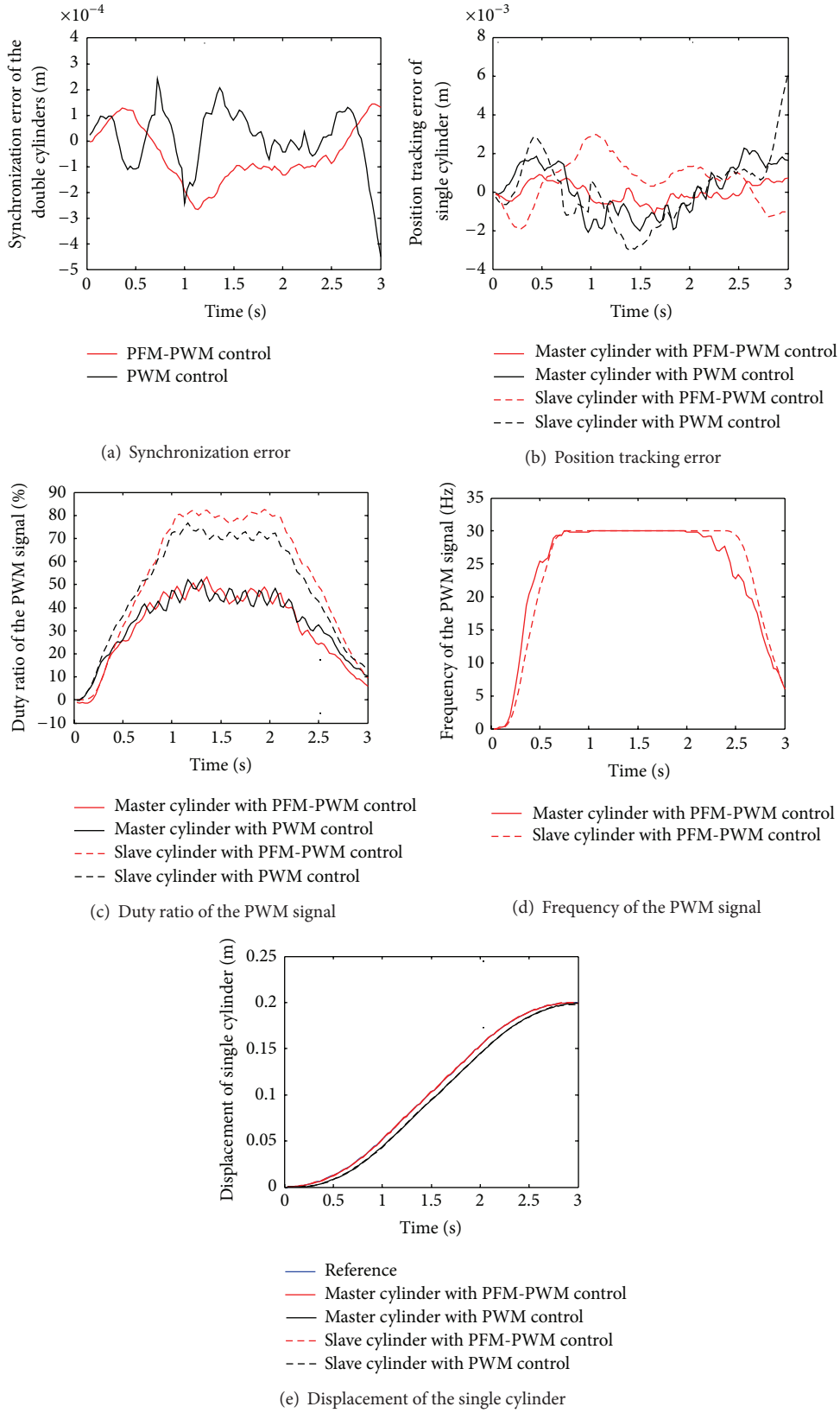

Figure 21: Experimental verification of collaborative synchronization control and PWM-PFM control.

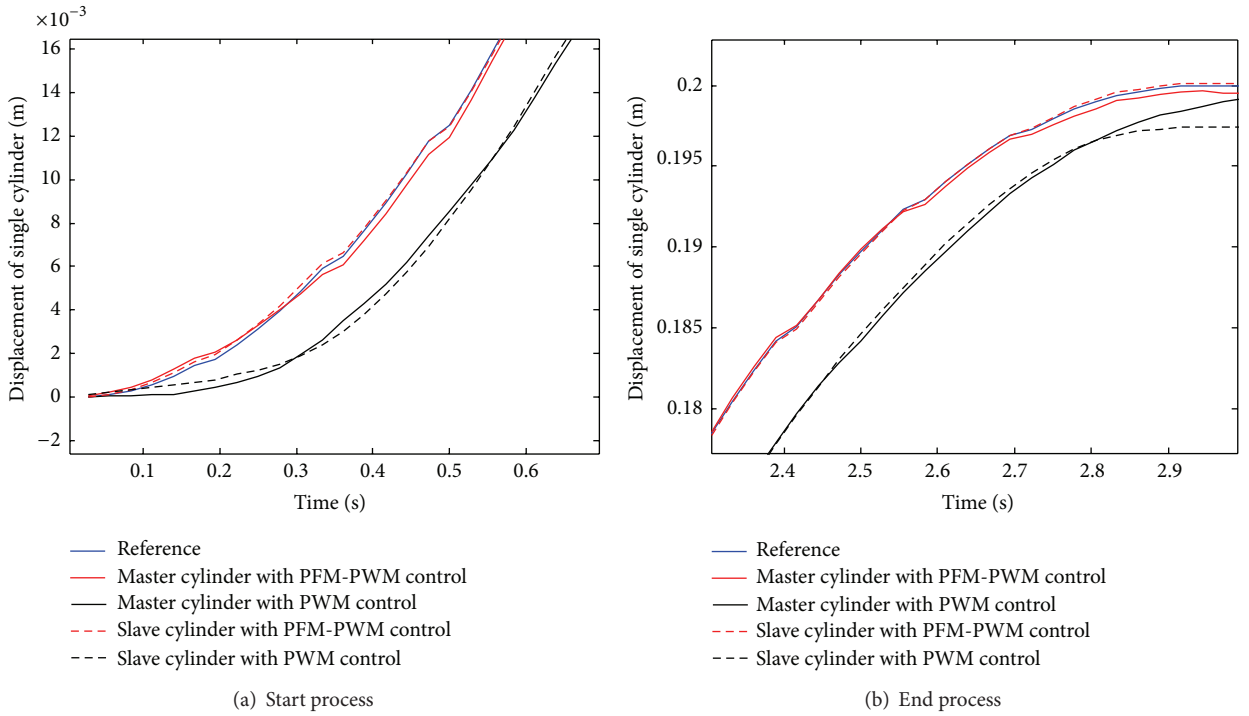

Figure 22: Magnified displacement of the single cylinder.

control is done and the result is shown in Figure 21, and the magnified displacement of the single cylinder is presented to distinguish the difference of different control clearly (Figure 22).

Figures 21-22 show that (1) with the PWM-PFM, the position tracking error of the master cylinder is limited to 1 mm and the position tracking error of the slave cylinder is decreased to 2.5 mm.

(2) HSV with PWM-PFM control can decrease the position tracking error and achieve the precise position control of the single hydraulic cylinder.

(3) Fuzzy algorithm and HSV with PWM-PFM are effective to eliminate the displacement error between the double cylinders which results from the different load environment and the synchronization error is limited in 0.15 mm.

6. Conclusions

The application of synchronization control of the double hydraulic cylinder controlled directly by HSV is proposed to solve the problem of hydraulic synchronization system that synchronous precision is not high. The flow characteristic of HSV is researched by mathematical analysis and the flow characteristics of PWM and PWM-PFM are analyzed and compared with each other. The collaborative synchronization control algorithm and collaborative synchronization control algorithm and PWM-PFM are validated by simulation and experiment.

The result implies that (1) HSV with PWM-PFM can have the linear relationship between the past flow and the duty ratio; (2) collaborative synchronization control algorithm and PWM-PFM can achieve the high precision synchronization control and limited the error to 0.15 mm.

The design methodology and control algorithm can be applied to other hydraulic systems with synchronization control requirement.

Conflict of Interests

The authors declare that there is no conflict of interests regarding the publication of this paper.

Acknowledgments

This study is supported by National Natural Science Foundation of China (Grant No.51475462).

References

[1] H. L. Gao and Y. Sang, "Discuss on synchronization control and its typical application," *Hydraulic Pneumatics & Seals*, vol. 5, pp. 1–7, 2012.

[2] H. Sun and G. T.-C. Chiu, "Motion synchronization for dual-cylinder electrohydraulic lift systems," *IEEE/ASME Transactions on Mechatronics*, vol. 7, no. 2, pp. 171–181, 2002.

[3] Q. Gao, H. Song, Z. Liu, T. Dong, and Z. Yang, "Research on speed control in starting and stopping processes of hydraulic cylinder with HSV," *China Mechanical Engineering*, vol. 24, no. 1, pp. 47–51, 2013.

[4] F. Wang, L. Gu, and Y. Chen, "A hydraulic pressure-boost system based on high-speed on-off Valves," *IEEE/ASME Transactions on Mechatronics*, vol. 18, no. 2, pp. 733–743, 2013.

[5] M. R. Adeli and H. Kakahaji, "Modeling and position sliding mode control of a hydraulic actuators using on/off valve with PWM technique," in *Proceedings of the 3rd International Students Conference on Electrodynamics and Mechatronics (SCE '11)*, pp. 59–64, October 2011.

[6] M. Taghizadeh, A. Ghaffari, and F. Najafi, "Improving dynamic performances of PWM-driven servo-pneumatic systems via a novel pneumatic circuit," *ISA Transactions*, vol. 48, no. 4, pp. 512–518, 2009.

[7] M. Sorli and S. Pastorelli, "Performance of a pneumatic force controlling servosystem: influence of valves conductance," *Robotics and Autonomous Systems*, vol. 30, no. 3, pp. 283–300, 2000.

[8] H. Qin, L. Gu, and Y. Chen, "Velocity control system for high inertia loads based on switch mode hydraulic power supply," *Chinese Journal of Mechanical Engineering*, vol. 40, no. 9, pp. 106–110, 2004.

[9] H. Sun, *Motion synchronization of multi-cylinder electro-hydraulic lift [Ph.D. thesis]*, Purdue University, 2001.

[10] Y. M. Fang, L. Zhao, and F. Ou, "Robust dynamic output feedback synchronous control for both sides of pressing down position system for cold rolling mill," *Acta Automatica Sinica*, vol. 35, no. 4, pp. 438–442, 2009.

[11] Z. Liu, "Simulation and design on high precision synchronization system of hydraulic lifting mechanism," *Manufacturing Technology & Machine Tool*, vol. 12, pp. 67–70, 2010.

[12] S. Mastellone, D. Lee, and M. Spong, "Master-slave synchronization with switching communication through passive model-based control design," in *Proceedings of the American Control Conference*, Minneapolis, Minn, USA, June 2006.

[13] Z. H. Liu, Q. H. Gao, and H. L. Niu, "The position control of the hydraulic cylinder controlled by the high-speed on-off valve," *Sensors and Transducer*, vol. 160, no. 12, pp. 590–601, 2013.

[14] E. E. Topçu, I. Yüksel, and Z. Kamiş, "Development of electro-pneumatic fast switching valve and investigation of its characteristics," *Mechatronics*, vol. 16, no. 6, pp. 365–378, 2006.

[15] L. Zhizhen, Z. Zhongxiang, and N. Xiaotao, "Second modulate method of the high speed on-off electromagnetic valve and its application to pressure regulating valves," in *Proceedings of the 33rd Annual Conference of the IEEE Industrial Electronics Society (IECON '07)*, pp. 534–538, Taipei, Taiwan, November 2007.

[16] Ž. Šitum, T. Žilić, and M. Essert, "High speed solenoid valves in pneumatic servo applications," in *Proceedings of the Mediterranean Conference on Control and Automation (MED '07)*, pp. 1–6, Athens-Greece, July 2007.

[17] Z. H. Liu, Q. H. Gao, and H. L. Niu, "The research on the position control of the hydraulic cylinder based on the compound algorithm of fuzzy & feedforward-feedback," *Sensors & Transducers*, vol. 161, no. 1, pp. 309–320, 2014.

[18] M. Shih and M. Ma, "Position control of a pneumatic cylinder using fuzzy PWM control method," *Mechatronics*, vol. 8, no. 3, pp. 241–253, 1998.

[19] O. Ekren, S. Sahin, and Y. Isler, "Comparison of different controllers for variable speed compressor and electronic expansion valve," *International Journal of Refrigeration*, vol. 33, no. 6, pp. 1161–1168, 2010.

[20] J. Zheng, S. Zhao, and S. Wei, "Application of self-tuning fuzzy PID controller for a SRM direct drive volume control hydraulic press," *Control Engineering Practice*, vol. 17, no. 12, pp. 1398–1404, 2009.